Evaluation of the Morphology and Malachite Green Absorption Capacity of Modified Electrospun Chitosan Nanofibers

Hien Thi Thanh Nguyen*, Thao Thi Ngoc Dang, Tan Minh Ha, and Nhi Tran Yen Nguyen

Faculty of Chemical Engineering, Ho Chi Minh City University of Industry and Trade, 140 Le Trong Tan Street, Tan Phu District, Ho Chi Minh City 700000, Vietnam

** Corresponding author:*

tel: +84-918141110
email: hienntt@huit.edu.vn

Received: August 4, 2024
Accepted: January 8, 2025

DOI: 10.22146/ijc.98911

Abstract: *This article studies the factors affecting the morphology of electrospun chitosan nanofibers modified with polyvinyl alcohol (PVA) and using formed nanofibers for malachite green (MG) adsorption. Chitosan concentrations of 2 and 3 wt.% combined with PVA, the nanofibers are formed with sizes under 75 nm, in contrast to the results of the chitosan solutions formed particles. This result is due to the interaction between the functional group of the polymers that increases entanglement. Machine operating and polymer solution parameters affect the nanofiber morphology. Combining the principal component analysis (PCA) method and physicochemical analysis showed that the factors of chitosan solution, such as concentration, viscosity, and conductivity, mainly influenced the fiber formation process. Besides, the initial test results of CTS 3 wt.%/PVA (1:1) nanofibers adsorbing MG at 10 mg/L concentration exhibited a high adsorption performance (more than 89%), and the amount of absorbed dye (35.83 mg/g) after 120 min at pH 6.8. The obtained results will be worth information for creating chitosan nanofibers by electrospinning the next time and evaluating the MG adsorption capacity of chitosan nanofibers in the presence of PVA.*

Keywords: *chitosan nanofibers; electrospinning; adsorption; malachite green*

■ INTRODUCTION

The vigorous development of nanofiber materials has promoted diverse research on these materials, including methods, properties, and applications. The outstanding characteristic of nanomaterials is their nano size, so they have a high surface area to volume ratio that improves features like solubility and adsorption capacity compared to large-sized materials. Therefore, the number of publications on nanofibers is increasing quickly [1-4]. In particular, the procedure of creating nanofibers by electrospinning is considered in terms of effectiveness and simplicity due to the ease of operation, use of less solvents, ensuring product integrity, and one-step operation [4-7]. Polymers are often chosen as materials for forming electrospun nanofibers [3,5]. Among those environmentally friendly polymers that are paid attention to are chitosan (CTS), cellulose, polylactic acid, alginate, and polyvinyl alcohol (PVA). CTS is a type of polysaccharide owing to many advantages: being easy to produce, less toxic, compatible, and biodegradable. More specifically, the structure of CTS has many functional groups, so it can be easily modified to improve its properties [7-8]. Many materials, such as PVA, cellulose, and polyethylene glycol, are modified with CTS based on the interaction of functional groups, as published [5,7-11]. Especially in the field of application as an adsorbent, CTS nanofibers are often modified to increase the mechanical strength and wetting ability [12-14].

However, the morphology of electrospun nanofibers formed requires control of two main factors: machine parameters (distance electrode distance, voltage, flow) and polymer solution parameters (concentration, viscosity, conductivity) [3,5,15]. Therefore, finding the main factors affecting fiber morphology is always necessary. This article uses several characterization techniques and the value of viscosity and conductivity of polymer solutions to analyze the

physicochemical characteristics combined with machine operating parameters and the principal component analysis (PCA) statistical method to clarify crucial factor influence on morphology nanofiber formation [16]. The combination of the results of physicochemical analysis and statistical analysis increases the reliability of the results obtained.

Besides, the formed nanofibers were tested to adsorb malachite green (MG), which is used in large quantities in practice as a dye in the leather, shoe, paper, wool, and cotton industries, especially in the aquaculture as an antiseptic, fungicide, therapeutic agent. However, MG is difficult to decompose, and if its excess in water sources becomes a potential source of toxicity. It can enter into the human system via the food chain, which causes harmful effects like cancer and genetic mutations [17-20]. Therefore, the study wants to rely on the good characteristics of nanofiber materials as an excellent adsorbent for treating MG.

■ EXPERIMENTAL SECTION

Materials

CTS originated from Vietnam, and PVA (the degree of polymerization in 1700–1800, 98% hydrolyzed) was purchased from Oxford (India). MG was obtained from Xilong (China). All the chemicals were of analytical reagent grade without further purification.

Instrumentation

Electrospinning apparatus

An electrospinning system consists of three major components: a high-voltage power supply, a syringe pump containing a nozzle, and a nanofiber rotating drum collector (with a rotation speed of 500 rpm). For the fabrication of nanofibers, the polymer solution was pushed to the nozzle by a syringe pump. Then, applying a high voltage at the nozzle and the collector (as two electrodes), the droplet on the nozzle is charged and thus turns into a droplet's Taylor cone shape [15]. After that, the electrostatic repulsive forces increase and overcome the forces of surface tension. Thin jets of the tip of the cone are stretched in a straight line and then undergo strong whisking movements while transferring toward the collector due to the instability of the curvature. The rapid evaporation of the solvent occurs in the road moving toward the collector, so the solid nanofibers are rolled along the rotating drum collector surface.

Characterization instrumentations

Structures of the polymer were analyzed by Fourier-transform infrared spectroscopy (FTIR) on a Frontier of Perkin Elmer spectrophotometer. The polymers were mixed with KBr and pressed to a plate for measurement. The crystalline phase of chitosan's was measured by X-ray diffraction (XRD, D2 Phaser, Bruker). The spectrometry's were obtained by using the powder diffraction meter with Cu-Ka radiation in the 2θ range of 5–70°. The viscosity and conductivity of the solution were determined by the Brookfield Gel Timer Instrument viscometer and WTW inoLab® Cond 7310 at 30 °C. The surface morphology of nanofiber was studied by scanning electron microscopy (SEM, S4800 HITACHI). Size distributions of the nanofibers were randomly selected with diameters of 50 nanofibers from each sample, and they were analyzed using ImageJ and Minitab software.

Procedure

Fiber formation via electrospinning

CTS was dissolved in 90 wt.% aqueous acetic acid at room temperature to obtain 2, 3, and 4 wt.% concentrations. In addition, the PVA solution was prepared by dissolving PVA in deionized water (10% w/v) at 90 °C. All the solutions were stirred to make homogeneous solutions. Then, both solutions were mixed with volume ratios (CTS/PVA) of 1:1, 1:2, 1:3, and 1:4. The final solutions were transferred into an electrospinning system. The operation parameters like flow rate (Q), voltage (U), and distance from the nozzle tip to the collector (L) were investigated in a range of 0.1–1.0 mL/h, 9–18 kV, and 7–12 cm, respectively. Meanwhile, the collector speed (S) was firmly set to 500 rpm, and the used nozzle was an 18-gauge stainless steel needle (inner diameter 0.838 mm).

Adsorption experiments

The exactly weighted absorbent was immersed in aqueous MG solutions (10 mg/L) at specific periods under

room temperature and pH of distilled water (6.8) and pH 8.0, respectively. Residual concentrations of MG in the solution were determined by measuring absorbance spectrophotometrically at 614 nm [21-23]. The adsorption capacity Q (mg/g) and percentage adsorption of dyes H (%) in the fibers were calculated based on Eq. (1) and (2);

$$Q = \frac{V(C_0 - C_t)}{m} \quad (1)$$

$$H = \frac{C_0 - C_t}{C_0} \times 100\% \quad (2)$$

where V is the total volume of the solution (L), C_0 and C_t are the initial dye concentration and the remaining dye concentration (mg/L), respectively, and m is the weight of the adsorbent (g).

Statistical analysis

All modes of working combined between the parameters of chitosan solution and electrospinning machine obtained with nanofiber morphology by SEM analysis in this study were subjected to PCA analysis by Minitab software.

■ RESULTS AND DISCUSSION

Parameters Affecting the Morphology of Electrospun CTS Nanofibers

CTS was selected with physicochemical characteristics: deacetylation degree (DD) higher than 80% and average molecular weight of 516 kDa, as demonstrated in the previous work [24]. According to the literature [3,15], polymers possessing enormous molecular weight, high viscosity, and high entanglement are suitable for creating fibers by electrospinning. So, the CTS owns many NH_2 groups in the structure, causing repulsion of positive charges in a solvent, which leads to considerable expansion of polymer chains and the extent of molecular entanglement of the polymer. Besides, a high molecular weight creates high viscosity, proportional to the polymer chain length. All these predict that CTS is suitable for fiber formation.

CTS concentration

All experimented CTS concentrations in 90 wt.% acetic acid show mostly no electrospun nanofibers in SEM images in Fig. 1(a-c) that exhibit nanoparticles or bead fibers. This may be mainly related to the concentration of entanglement. According to previous work [3,5-6,15], the chain entanglement must be large enough to form strong nanofibers because the polymer disentangles during stretching with few entanglements per chain. So, the polymer concentration has to exceed 2.0–2.5 times the entanglement concentration. The viscosity of the solution is a factor that influences the entanglement concentration. The higher the viscosity is, the more increasing entanglement. In fact, CTS concentrations of 2, 3, and 4 wt.% obtained viscous values of 476, 631, and 1776 cP, correspondingly. Especially at a concentration of 4%, the viscosity increases quickly as a sign of over-entanglement concentration, leading to the appearance of some thin fibers in the SEM image in Fig. 1(c). Unfortunately, the electrospinning process at this concentration was complicated due to the nozzle being solidified and blocked. So, it can be said that the interchain connectivity via chain entanglements in the structure of chitosan needs to improve in the range of 2 to 3 wt.% concentration without increasing the viscosity too high to perform electrospinning. PVA was added to the chitosan solution to enhance this property.

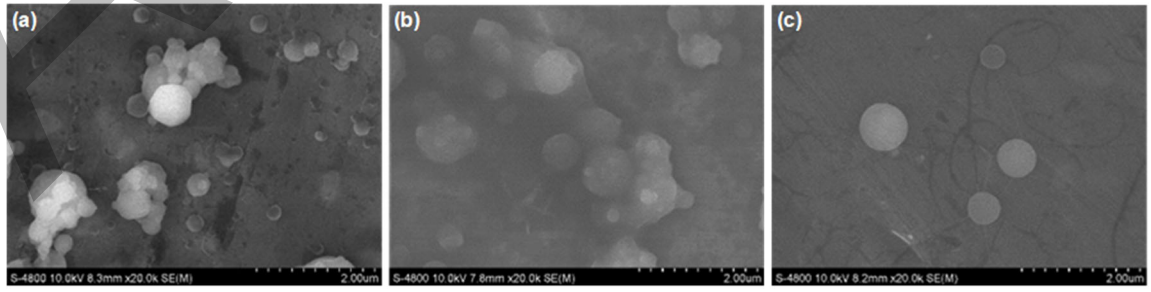

Fig 1. SEM images of electrospun CTS at concentrations of (a) 2, (b) 3, and (c) 4 wt.%

Content of PVA

The presence of PVA in CTS according to volume ratio (1:1, 1:2, 1:3, and 1:4) shows all the formation of nanofibers with diameters smaller than 422 nm of pure PVA in Fig. 2(a-f) at different modes of electrospinning operation. However, the size and uniformity of the fibers are different. In detail, the average diameter of nanofibers of 2 wt.% CTS is no significant difference between 56 and 58 nm corresponding ratios of CTS/PVA 1:1 and 1:2 in Fig. 2(b) and 2(c). The uniformity of these fibers is not high. They are mainly the bead-on-string structure. Whereas the remaining samples of 3 wt.% CTS obtained an average diameter below 75 nm, and especially the CTS 3 wt.%/PVA (1:1) and CTS 3 wt.%/PVA (1:4) samples have high uniformity, smoothness, and diameter of 68 and 48 nm (Fig. 2(e) and 2(f)). Generally, only CTS 3 wt.%/PVA (1:4) obtained nanofibers without beads.

Fig. 3 and 4 show the viscosity and conductivity of the CTS/PVA polymer solution higher than that of each pure solution and increased with CTS concentration and the content of PVA. Specifically, the concentration of CTS 3 wt.%/PVA (1:4) solution reached the largest value of viscosity and conductivity of 1341 cP and 1067 µS/cm.

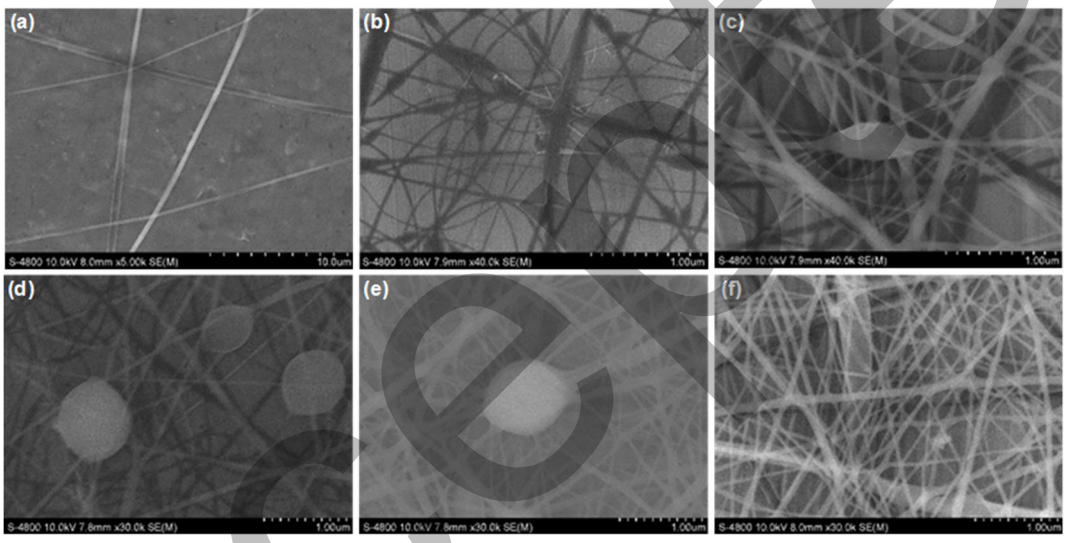

Fig 2. SEM image of (a) PVA, (b) CTS 2 wt.%/PVA (1:1), (c) CTS 2 wt.%/PVA (1:2), (d) CTS 3 wt.%/PVA (1:1), (e) CTS 3 wt.%/PVA (1:3), and (f) CTS 3 wt.%/PVA (1:4)

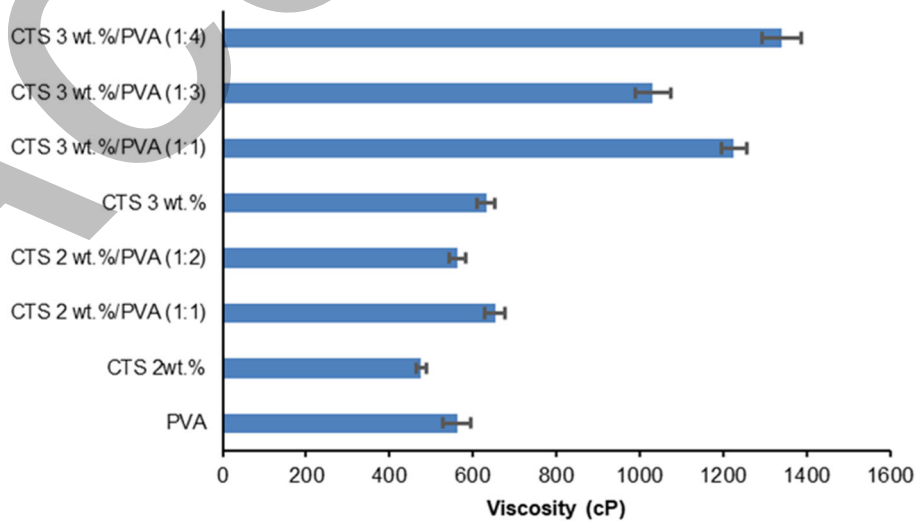

Fig 3. Viscosity of the polymer solutions

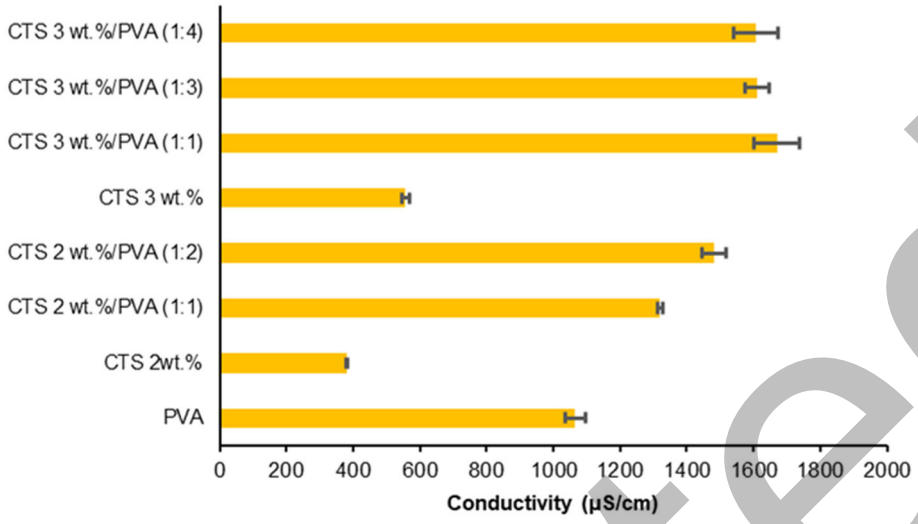

Fig 4. Conductivity of polymer solutions

Meanwhile, 2 wt.% CTS concentration has the smallest values of 467 cP and 382 µS/cm, respectively. This predicts that there is an interaction between CTS and PVA structures.

The higher the CTS concentration, the greater the number of functional groups, so more hydrogen-bonding interaction with PVA functional groups leads to increased viscosity. Besides, a high CTS concentration contains more positive charge in an acidic solution, and mixing the two polymer solutions makes a dilute aqueous acid acetic solution, thus enhancing the conductivity of solutions. The FTIR spectrum also demonstrates the change in intensity and wavelength position of characteristic peaks when polymers are combined, as shown in Fig. 5.

The FTIR spectra of CTS, PVA, and CTS/PVA display the characteristic groups of polymers and their interactions (Fig. 5). The CTS owns representative peaks, including the broadband (3300–3600 cm^{-1}) corresponding to both $–NH_2$ and –OH groups showing the intramolecular hydrogen bonds, the absorption peaks of C=O group (amide type 1) at 1650 cm^{-1} and the NH group (amide type 2) at 1590 cm^{-1}. Similarly, all major peaks related to hydroxyl and acetate groups of PVA are observed. The sharp peak at 3603 cm^{-1} refers to absorption corresponding to the –OH stretching, and the weak peaks at 1699 cm^{-1} are associated with stretching vibrations of C=O bonds present in a few acetate units in the polymer chain by high hydrolysis degrees. For the CTS/PVA fibers,

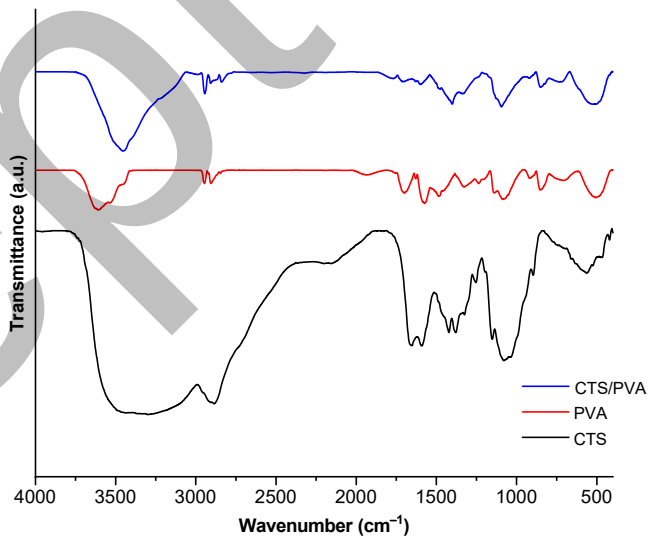

Fig 5. FTIR spectra of the polymers

the –C=O and N–H absorption peaks are very similar to the CTS spectra, but the intensity is lower and shifted to higher wavelengths of 1704 and 1598 cm^{-1}, respectively. It implies that the interaction of the functional groups. In addition, the strong band of the –OH group is less broad than those of CTS, and the wavenumber center shifted between initial wavenumbers of PVA and CTS (3461 cm^{-1}). It can be inferred that extensive intermolecular hydrogen bonds between the PVA and CS chains were formed.

As shown in the results of the XRD spectra in Fig. 6, CTS has a large degree of crystallinity, presenting a characteristic peak at 2θ around 20° (amine II, $–NH_2$), a

high intensive peak at 10° (amine I, –N–CO–CH_3), and an additional shoulder in 21° [25]. PVA had a sharp intensity diffraction peak at 2θ ≈20° which corresponded to the crystalline structure, and low-intensity peaks at the diffraction angle of 12° and 41°. However, the XRD pattern of CTS/PVA exhibited only a low-intensity peak at 2θ around 20° of an amorphous phase. Significantly, the peak at 2θ ≈12°, 41° in the XRD curve of pure PVA and 2θ ≈10° of pure CTS almost disappeared. This is mainly attributed to the weakening of the intramolecular forces inside the polymers, which reflects an increase in amorphous phases. Thus, it can be said that the XRD patterns illustrate intermolecular hydrogen bonds of $H_2N\cdots OH$ and $CHO\cdots OH$ between the PVA and CTS chain.

Operating parameters

The polymer solutions were investigated following a change of voltage (U), distance from the nozzle to the collector (L), and flow rate (Q). In general, the rule of influence of U and L factors follows the previous work in that the appropriate of them perfectly creates a strong electric field force to pull the droplet at the tip of the nozzle as cone shape to the collection drum and evaporate most of the solvent on the way [6,26]. The shapes of droplets at the nozzle tip of the same distance (L = 10 cm) are photographed by a microscope in Fig. 7. When the potential voltage is small (U = 12 kV), the droplet at the tip of the needle is large as a dripping shape (Fig. 7(a)) because the electric field force is not strong enough to remove the liquid.

As the voltage increased (U = 15 and 18 kV), the droplet is elongated and shaped like a cone shape (Fig. 7(b) and 7(c)), which can make the nanofiber. All obtained nanofibers were processed around 15–18 kV and a distance of 7–10 cm. For Q, the results at a high flow rate of 1 mL/h showed overlapping wet patches on the collection due to insufficient time for solvent evaporation. In contrast, with two low flow rates of 0.1 and 0.5 mL/h, the fibers formed of CTS 3 wt.%/PVA (1:4) have a similar average size of 43 and 48 nm in Fig. 8(a) and 8(b).

PCA Analysis

Seven parameters of process formation of the electrospun nanofibers, including U, L, Q, CTS concentration, ratio of CTS/PVA, viscosity, and conductivity of polymer solutions, were investigated. The database contained 15 records that can form nanofiber (diameter under 500 nm illustrated by the SEM images). The results of Table 1 show that the eigenvalue of the covariance matrix has the first three principal components with a cumulative total of 81%. Therefore, it is considered an appropriate level of variation that can be explained in the data. Among them, the first two principal components have eigenvalues greater than 1. Additionally, the first principal component (PC1)

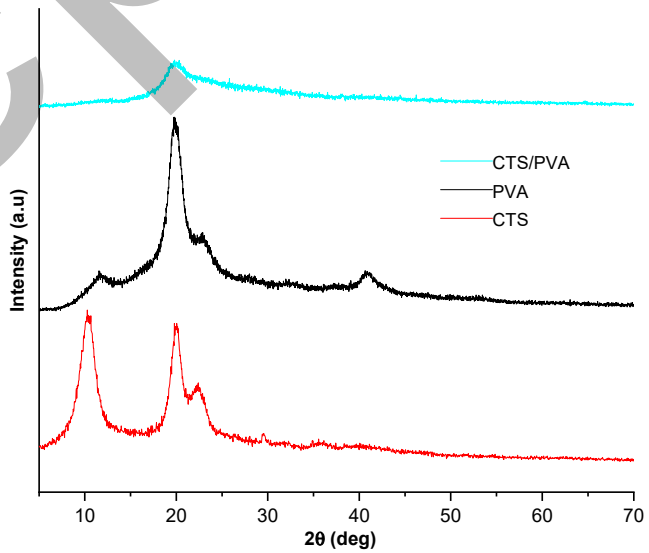

Fig 6. XRD spectra of the polymers

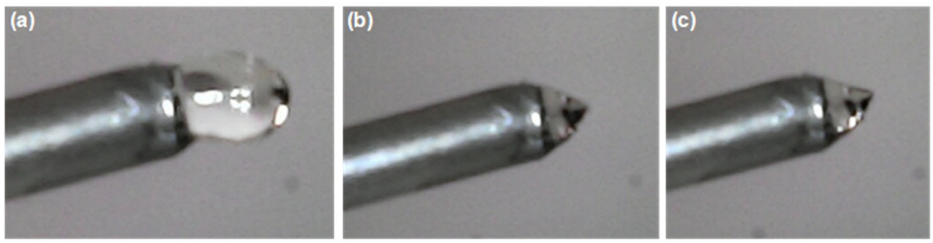

Fig 7. Images of the droplets at the nozzle tip of (a) U = 12 kV, (b) U = 15 kV, and (c) U = 18 kV

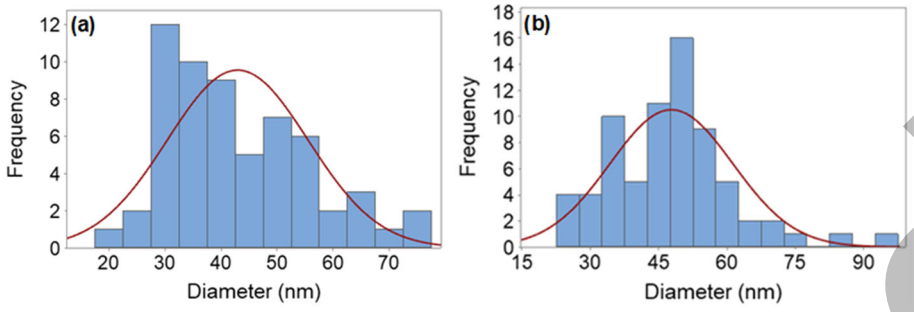

Fig 8. Size distribution curve of nanofibers of CTS 3 wt.%/PVA (1:4) at (a) 0.1 and (b) 0.5 mL/h

Table 1. Eigen analysis of the correlation matrix

Eigenvalue	3.370	1.365	0.935	0.783	0.305	0.221	0.022
Proportion	0.481	0.195	0.134	0.112	0.043	0.032	0.003
Cumulative	0.481	0.676	0.810	0.922	0.965	0.997	1.000

accounts for 48.1% of the total variance of the dataset, whereas the second and third hold in the order to 19.5 and 13.4%, respectively.

In Fig. 9, the variables most correlated with the PC1 are conductivity, CTS concentration, and viscosity, corresponding to the vector values to decrease in order 0.524, 0.523, and 0.481. The PC1 has strong positive associations with all three variables. Therefore, increasing these variable values will increase the value of PC1. This component primarily measures the factors of the CTS solution. For the second principal component (PC2), the positive correlation of the ratio of CTS/PVA obtains the highest vector value of 0.654. It is also a polymer solution feature. The flow rate presented the highest negative correlation with the third principal component (PC3). It can be said that the properties of CTS solution strongly impact morphology fibers, in contrast to the operation parameters. Combined physicochemical and PCA analysis exhibits the factors of polymer solution that need much attention in the case of creating chitosan nanofibers by the electrospinning method the next time.

Adsorption of MG on Electrospun Chitosan Nanofibers

The CTS 3 wt.%/PVA (1:1) and CTS 3 wt.%/PVA (1:4) fiber samples showing the best morphology were used to test MG adsorption with a concentration of 10 mg/L, which is a maximum threshold threat to human health [20]. Firstly, at pH 6.8, with the CTS 3 wt.%/PVA (1:4) nanofiber adsorbent dosage in the 0.25–7.5 g/L range, the adsorption capacity and removal efficiency MG of the adsorbent in 60 min are presented in Fig. 10. The removal efficiencies of MG were the same

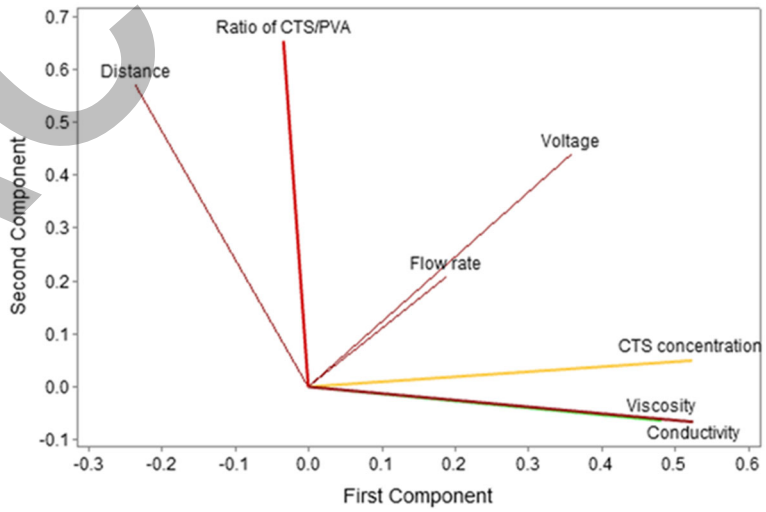

Fig 9. The loading plot of the first and the second component

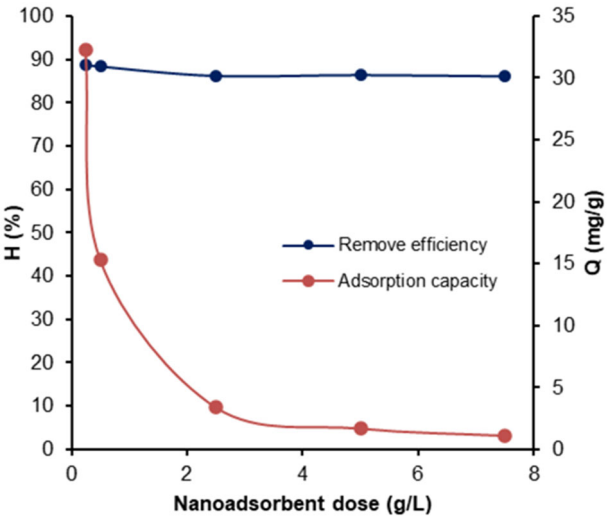

Fig 10. Effect of the content of CTS 3 wt.%/PVA (1:4) nanoadsorbent on adsorption capacity and removal efficiency

in the various content of the fibers, an average of 88.5%. However, the adsorption capacity Q decreased quickly from 32.3 to 1.15 mg/g with increasing adsorbent dosage. With an MG concentration of 10 mg/L, only a low amount of adsorbent of 0.25 g/L is needed to provide enough active centers to adsorb MG. The active center position can increase with high doses of absorbent. However, overlapping the active sites reduced the degree of contact between the nano adsorbents and MG or increased the distance for the diffusion pathway. That is the reason the removal efficiency did not improve.

Next, at the concentration of 0.25 g/L, the adsorption capacity MG of two nanofibers samples was displayed in Fig. 11. At pH 6.8, after 10 min, the dye adsorbed onto the CTS 3 wt.%/PVA (1:1) fibers obtained was 34.2%. It slightly increased and stabilized at 35.8% after 120 min. This means the adsorption process occurred quickly as a result of many active sites in the sample or forming interaction of MG and the fibers. In contrast, the adsorption capacity of CTS 3 wt.%/PVA (1:4) gradually increased from 32.1 to 32.3%, corresponding 10 to 60 min, and rising quickly to 35.8% after 120 min. This shows that the active sites may assemble at the location of CTS. A large amount of PVA can cover the active site in the matrix, causing the attraction of MG to the adsorbent to be prolonged.

The results of the MG adsorption at pH 8.0 trended the same at pH 6.8. The CTS 3 wt.%/PVA (1:1) sample showed good adsorption capacity (Q) in the first 10 min with a value of 22.5 mg/g and almost stabilized at 26.45 mg/g after 120 min. Meanwhile, in the CTS 3 wt.%/PVA (1:4) sample, the amount of absorbed dye increased from 1.1 to 25.8 mg/g, corresponding to adsorption time from 10 to 120 min. This result confirms that the structural arrangement of the CTS 3 wt.%/PVA (1:1) sample creates favorable conditions for MG adsorption.

The graph also indicated the MG adsorption capacity of nanofibers at pH 6.8 was better than at pH 8.0.

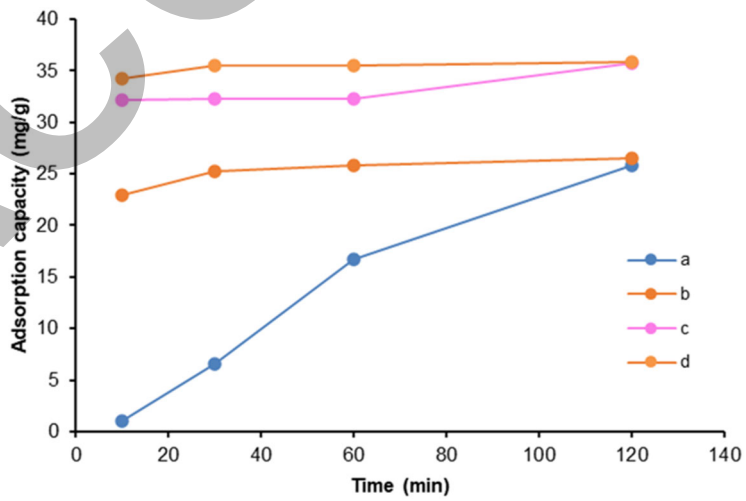

Fig 11. Change in adsorption capacity of fibers in time of CTS 3 wt.%/PVA(1:4) at pH (a) 6.8 and (c) 8.0 and CTS 3 wt.%/PVA(1:1) at pH (b) 6.8 and (d) 8.0

Generally, the solutions' pH mainly affects the dissociation/ionization of the functional groups of the fibers and MG. In pH 6.8, the formation of the $-NH_3^+$ ion of CTS created an electrostatic bonding with MG (pKa 6.9) that carried an anion charge at low pH [19]. In the case of pH 8.0, the positive charge of fibers deceased, resulting in electrostatic attraction.

■ CONCLUSION

The study examines the working modes of creating electrospun CTS/PVA nanofibers. With CTS concentration of 2 and 3 wt.% blending on PVA following the different ratios (1:1; 1:2; 1:3), the formed nanofibers had an average diameter below 75 nm and contained few beads on the strings. In particular, the CTS 3 wt.%/PVA (1:4) sample obtained smooth fibers and no beads with a size of 48 nm. The analysis of operation parameters, physicochemical characteristics of polymer solution, and PCA showed that the polymer solution parameters greatly determine the fiber morphology. The interaction between the functional groups of CTS and the PVA demonstrated through FTIR and XRD spectra, is the reason for the change in the properties of the polymer solution, including increasing entanglement, viscosity, and conductivity. Therefore, it facilitates the creation of nanofibers. Using CTS 3 wt.%/PVA nanofibers samples as the adsorbents of MG at a concentration of 10 mg/L gave a better result of pH 6.8 than of pH 8.0. The CTS 3 wt.%/PVA (1:1) nanofibers sample indicated the adsorption capacity of 35.8 mg/g after 120 min at pH 6.8. The presence of PVA in the structure of CTS can reduce the diffusion of MG or hide the active sites. It will be an interesting topic that needs further research in adsorption.

■ ACKNOWLEDGMENTS

The authors thank the support of facilities from Ho Chi Minh City University of Industry and Trade. This work was financially supported by Ho Chi Minh City University of Industry and Trade under Contract no 89/HĐ-DCT dated 15 Aug 2023.

■ CONFLICT OF INTEREST

All the authors declare that they have no conflict of interest.

■ AUTHOR CONTRIBUTIONS

Thao Thi Ngoc Dang, Tan Minh Ha, and Nhi Tran Yen Nguyen: support for doing experiments and handling data. Hien Thi Thanh Nguyen: methodology, experiment, data management, supervision, writing, editing, and manuscript completion. All authors have read and agreed to the final version of the manuscript.

■ REFERENCES

[1] Nasrollahzadeh, M., Sajadi, S.M., Sajjadi, M., and Issaabadi, Z., 2019, "Applications of Nanotechnology in Daily Life" in *Interface Science and Technology*, Academic Press, Cambridge, MA, US, 113–143.

[2] Findik, F., 2021, Nanomaterials and their applications, *Period. Eng. Nat. Sci.*, 9 (3), 62–75.

[3] Islam, M.S., Ang, B.C., Andriyana, A., and Afifi, A.M., 2019, A review on fabrication of nanofibers via electrospinning and their applications, *SN Appl. Sci.*, 1 (10), 1248.

[4] Ali, S.H., Mahammed, M.A., and Yasin, S.A., 2024, Characterization of electrospinning chitosan nanofibers used for wound dressing, *Polymers*, 16 (14), 1984.

[5] Xue, J., Wu, T., Dai, Y., and Xia, Y., 2019, Electrospinning and electrospun nanofibers: Methods, materials, and applications, *Chem. Rev.*, 119 (8), 5298–5415.

[6] Geng, X., Kwon, O.H., and Jang, J., 2005, Electrospinning of chitosan dissolved in concentrated acetic acid solution, *Biomaterials*, 26 (27), 5427–5432.

[7] Salas, C., Thompson, Z., and Bhattarai, N., 2017, "Electrospun Chitosan Fibers" in *Electrospun Nanofibers*, Woodhead Publishing, Cambridge, MA, US, 371–398.

[8] Cheba, B.A., 2020, Chitosan: Properties, modifications and food nanobiotechnology, *Procedia Manuf.*, 46, 652–658.

[9] Xu, J., Zhang, J., Gao, W., Liang, H., Wang, H., and Li, J., 2009, Preparation of chitosan/PLA blend micro/nanofibers by electrospinning, *Mater. Lett.*, 63 (8), 658–660.

[10] Cheng, Y., Farasati Far, B., Jahanbakhshi, M., Bahrami, S., Tamimi, P., Sedaghat, M., and Ghazizadeha, E., 2023, Exploring the potential of a polyvinyl alcohol/chitosan-based nanofibrous matrix for erythromycin delivery: Fabrication, *in vitro* and *in vivo* evaluation, *RSC Adv.*, 13 (27), 18450–18460.

[11] Choo, K., Ching, Y.C., Chuah, C.H., Julai, S., and Liou, N.S., 2016, Preparation and characterization of polyvinyl alcohol-chitosan composite films reinforced with cellulose nanofiber, *Materials*, 9 (8), 644.

[12] Lou, T., Yan, X., and Wang, X., 2019, Chitosan coated polyacrylonitrile nanofibrous mat for dye adsorption, *Int. J. Biol. Macromol.*, 135, 919–925.

[13] Sakib, M.N., Mallik, A.K., and Rahman, M.M., 2021, Update on chitosan-based electrospun nanofibers for wastewater treatment: A review, *Carbohydr. Polym. Technol. Appl.*, 2, 100064.

[14] Phan, D.N., Lee, H., Huang, B., Mukai, Y., and Kim, I.S., 2019, Fabrication of electrospun chitosan/cellulose nanofibers having adsorption property with enhanced mechanical property, *Cellulose*, 26 (3), 1781–1793.

[15] Sasmazel, H.T., and Ozkan, O., 2013, Advances in electrospinning of nanofibers and their biomedical applications, *Curr. Tissue Eng.*, 2 (2), 91–108.

[16] Younes, K., Mouhtady, O., Chaouk, H., Obeid, E., Roufayel, R., Moghrabi, A., and Murshid, N., 2021, The application of principal component analysis (PCA) for the optimization of the conditions of fabrication of electrospun nanofibrous membrane for desalination and ion removal, *Membranes*, 11 (12), 979.

[17] Chen, Z.Y., He, B., Bian, Y., Zhang, Y., and Feng, X., 2024, Malachite green and related substances in environmental samples: Updates on pretreatment and analysis methods, *J. Environ. Chem. Eng.*, 12 (5), 113812.

[18] Abubakar, H.L., Tijani, J.O., Abdulkareem, A.S., Egbosiuba, T.C., Abdullahi, M., Mustapha, S., and Ajiboye, E.A., 2023, Effective removal of malachite green from local dyeing wastewater using zinc-tungstate based materials, *Heliyon*, 9 (9), e19167.

[19] Oladoye, P.O., Ajiboye, T.O., Wanyonyi, W.C., Omotola, E.O., and Oladipo, M.E., 2023, Insights into remediation technology for malachite green wastewater treatment, *Water Sci. Eng.*, 16 (3), 261–270.

[20] Gavrilenko, N.A., Volgina, T.N., Pugachev, E.V., and Gavrilenko, M.A., 2019, Visual determination of malachite green in sea fish samples, *Food Chem.*, 274, 242–245.

[21] Kamath Miyar, H., Pai, A., and Goveas, L.C., 2021, Adsorption of malachite green by extracellular polymeric substance of *Lysinibacillus* sp. SS1: Kinetics and isotherms, *Heliyon*, 7 (6), e07169.

[22] Naser, J.A., Al-ani, F.A.A., Radhi, I.M., and Himdan, T.A., 2020, Kinetic study of adsorption of malachite green dye on poly aniline-formaldehyde/chitosan composite, *IOP Conf. Ser.: Mater. Sci. Eng.*, 928 (5), 052005.

[23] Abou-Gamra, Z.M., and Ahmed, M.A., 2015, TiO_2 nanoparticles for removal of malachite green dye from waste water, *Adv. Chem. Eng. Sci.*, 5 (3), 373–388.

[24] Nguyen, H.T.T., Tran, T.N., Ha, A.C., and Huynh, P.D., 2022, Impact of deacetylation degree on properties of chitosan for formation of electrosprayed nanoparticles, *J Nanotechnol*, 2022 (1), 2288892.

[25] Jampafuang, Y., Tongta, A., and Waiprib, Y., 2019, Impact of crystalline structural differences between α-and β-chitosan on their nanoparticle formation via ionic gelation and superoxide radical scavenging activities, *Polymers*, 11 (12), 2010.

[26] Chinnappan, B.A., Krishnaswamy, M., Xu, H., and Hoque, M.E., 2022, Electrospinning of biomedical nanofibers/nanomembranes: Effects of process parameters, *Polymers*, 14 (18), 3719.